(2)

AD-A250 331

...RT DOCUMENTATION PAGE

1a.

1b. RESTRICTIVE MARKINGS

2a.

3. DISTRIBUTION/AVAILABILITY OF REPORT
Approved for public release; distribution unlimited.

2b. DECLASSIFICATION/DOWNGRADING SCHEDULE

MAY 1 2 1992

4. PERFORMING ORGANIZATION REPORT NUMBER(S)

5. MONITORING ORGANIZATION REPORT NUMBER(S)

6a. NAME OF PERFORMING ORGANIZATION	6b. OFFICE SYMBOL (If applicable)	7a. NAME OF MONITORING ORGANIZATION
Saint Louis University		Defense Advanced Research Projects Agency

6c. ADDRESS (City, State and ZIP Code)	7b. ADDRESS (City, State and ZIP Code)
221 North Grand Boulevard St. Louis, MO 63103	3701 N. Fairfax Drive Arlington, VA 22203-1714

8a. NAME OF FUNDING/SPONSORING ORGANIZATION	8b. OFFICE SYMBOL (If applicable)	9. PROCUREMENT INSTRUMENT IDENTIFICATION NUMBER
Defense Advanced Research Projects Agency	NMRO	FY3592-91-10651

8c. ADDRESS (City, State and ZIP Code)	10. SOURCE OF FUNDING NOS.			
	PROGRAM ELEMENT NO.	PROJECT NO.	TASK NO.	WORK UNIT NO.
3701 N. Fairfax Drive Arlington, VA 22203-1714				

11. TITLE (Include Security Classification) Attenuation & Source Studies in Norther Eurasia (unclassified)

12. PERSONAL AUTHOR(S)
Brian J. Mitchell

13a. TYPE OF REPORT	13b. TIME COVERED	14. DATE OF REPORT (Yr., Mo., Day)	15. PAGE COUNT
Semi-Ann. Technical	FROM 7/9/91 TO 1/8/92	1992 April 16	30

16. SUPPLEMENTARY NOTATION

17. COSATI CODES			18. SUBJECT TERMS (Continue on reverse if necessary and identify by block number)
FIELD	GROUP	SUB. GR.	Seismology, Attenuation, Lg, Surface waves

19. ABSTRACT (Continue on reverse if necessary and identify by block number)

Time series for Lg coda are being collected for numerous paths across a broad region of Eurasia, including the Barents shelf. To date we have collected seismograms generated by 30 earthquakes and 35 explosions and recorded at SRO, DWWSSN, and IRIS stations, as well as several stations of the former Soviet Union. A stacked spectral ratio method was applied to the coda of 85 Lg phases from those events to obtain values for Q and its frequency dependence at 1 Hz. Q values obtained so far vary between about 500 and 1000 and the frequency dependences range between 0.0 and 1.0.

Attenuation coefficient values of fundamental-mode Rayleigh waves determined for four two-station paths across the Basin and Range province fluctuate between about -2.0×10^{-3} km^{-1} and $+3.0 \times 10^{-3}$ km^{-1} at periods between 6 and 33 s. Particle motion plots

(continued)

20. DISTRIBUTION/AVAILABILITY OF ABSTRACT	21. ABSTRACT SECURITY CLASSIFICATION
UNCLASSIFIED/UNLIMITED ☒ SAME AS RPT. ☐ DTIC USERS ☐	

22a. NAME OF RESPONSIBLE INDIVIDUAL	22b. TELEPHONE NUMBER (Include Area Code)	22c. OFFICE SYMBOL
Dr. Alan Ryall	(703) 696-2245	

DD FORM 1473, 83 APR EDITION OF 1 JAN 73 IS OBSOLETE.

SECURITY CLASSIFICATION OF THIS PAGE

19. Abstract (continued)

indicate that many of those determinations are contaminated by arrivals from non-great circle paths and from waves generated at heterogeneities along the path. Attenuation coefficient determinations for the path MNV to ELK, which is approximately normal to structural trends in that region, are, however, relatively free from such contamination. Mean values for that path decrease rapidly with period from about 3.0×10^{-3} to about 0.7×10^{-3} km^{-1} between 6 and 10 s and then decrease slowly to about 0.3×10^{-3} km^{-1} at 33 s. Standard deviations range between 0.2×10^{-3} and 0.3×10^{-3} km^{-1} for most of the period range, but increase to about 0.4×10^{-3} at periods between 6 and 8 s. These results indicate that careful screening, based upon criteria such as three-dimensional particle motion, are necessary if surface wave attenuation data of sufficient quality to use for inverting for crustal anelasticity in complex regions are to be obtained.

ATTENUATION AND SOURCE STUDIES IN NORTHERN EURASIA

by

B.J. Mitchell
J.K. Xie
Y. Pan

Department of Earth and Atmospheric Sciences
Saint Louis University
221 North Grand Boulevard
St. Louis, MO 63103

10 April 1992

Semi-Annual Technical Report
9 July 1991 - 8 January 1992

TABLE OF CONTENTS

Contributing Scientists

B.J. Mitchell	Professor of Geophysics
J.K. Xie	Assistant Research Professor of Geophysics
Y. Pan	Graduate Student
W. Liu	Graduate Student

Publications

The following manuscript has been completed and submitted for publication. It describes difficulties, of which we should be aware, if fundamental-mode surface waves are utilized for yield determination, or detection and discrimination of nuclear events.

Mitchell, B.J., J. Xie, and W. Lin, Attenuation of multiphase surface waves in the Basin and Range province, part II: Fundamental-mode surface waves, Geophys. J. Int., submitted, 1992.

TECHNICAL SUMMARY

Time series for Lg coda are being collected for numerous paths across a broad region of Eurasia, including the Barents shelf. To date we have collected seismograms generted by 30 earthquakes ad 35 nuclear explosions and recorded at SRO, DWWSSN, and IRIS stations, as well as several stations of the former Soviet Union. A stacked spectral ratio method was applied to the coda of 85 Lg phases from those events to obtain values for Q and its frequency dependence at 1 Hz. Q values obtained so far vary between about 500 and 1000 and the frequency dependences range between 0.0 and 1.0.

Attenuation coefficient values of fundamental-mode Rayleigh waves determined for four two-station paths across the Basin and Range province fluctuate between about -2.0×10^{-3} km^{-1} and $+3.0 \times 10^{-3}$ km^{-1} at periods between 6 and 33 s. Particle motion plots indicate that many of those determinations are contaminaated by arrivals from non-great circle paths and from waves generated at heterogeneities along the path. Attenuation coefficient determinations for the path MNV to ELK, which is approximately normal to structural trends in that region, are, however, relatively free from such contamination. Mean values for that path decrease rapidly with period from about 3.0×10^{-3} to about 017×10^{-3} km^{-1} between 6 and 10 s and then decrease slowly to about 0.3×10^{-3} km^{-1} at 33 s. Standard deviations range between 0.2×10^{-3} and 0.3×10^{-3} km^{-1} for most of the period range, but increase to about 0.4×10^{-3} at periods between 6 and 8 s. These results indicate that careful screening based upon criteria such as three-dimensional particle motion, are necessary if surface wave attenuation data of sufficient quality to use for inverting for crustal anelasticity in complex regions are to be obtained.

RESEARCH RESULTS

I. Lg Attenuation in Northern Eurasia

Time series for Lg coda are continuing to be assembled for paths across northern Eurasia. To date, we have acquired records produced by 30 earthquakes and 35 nuclear explosions. The data cover a broad region of northern Eurasia, ranging from the Barents shelf, between Svalbard and Novaya Zemlya to a broad region of central Asia.

Data have been obtained from four sources: (1) SRO and DWWSS data from the U.S. Geological Survey, (2) Russian data from a collection of records at the Center for Seismic Studies (3) Russian data recorded by IRIS stations, and (4) Russian data, from Kirnos instruments, ordered through World Data Center B. The SRO, DWWSS, and IRIS data were available in digital form, but the other data were only available in analog form and had to be hand-digitized.

The stacked spectral ratio (SSR) method of Xie and Nuttli (1988) was applied to the coda of 85 Lg phases over a time interval between a group velocity of 3.1 km/s and at the time when the Lg coda becomes lost in noise. Since Lg coda is produced by scattered energy, it provides areal coverage rather than path coverage between sources and receivers. Xie and Mitchell (1990) approximated that coverage by ellipses with the source at one focus and the receiver at the other focus of this ellipse. Using that same approximation, late Lg coda, collected so far, provides the coverage shown in Figure 1.

The SSR method provides estimates of Q_o (Q at 1 Hz) and η (frequency dependence of Q) for the Lg coda. Q_o and η for the 85 Lg coda records so far analyzed yield values that range beetween about 500 and 1000 and between about 0.0 and 1.0, respectively.

There are still several time series to be digitized and analyzed. After completion of that task, we will apply Lg coda tomography (Xie and Mitchell, 1990) to the data to try to obtain regionalized maps of Q_o and η.

REFERENCES

Xie, J., and O.W. Nuttli Interpretation of high-frequency coda at large distances: stochastic modeling and method of inversion, *Geophys. J., 95,* 579-595, 1988.

Xie, J., and B.J. Mitchell, A back-projection method for imaging large-scale lateral variations of Lg coda Q with application to continental Africa *Geophys. J. Int., 100,* 161-181, 1990.

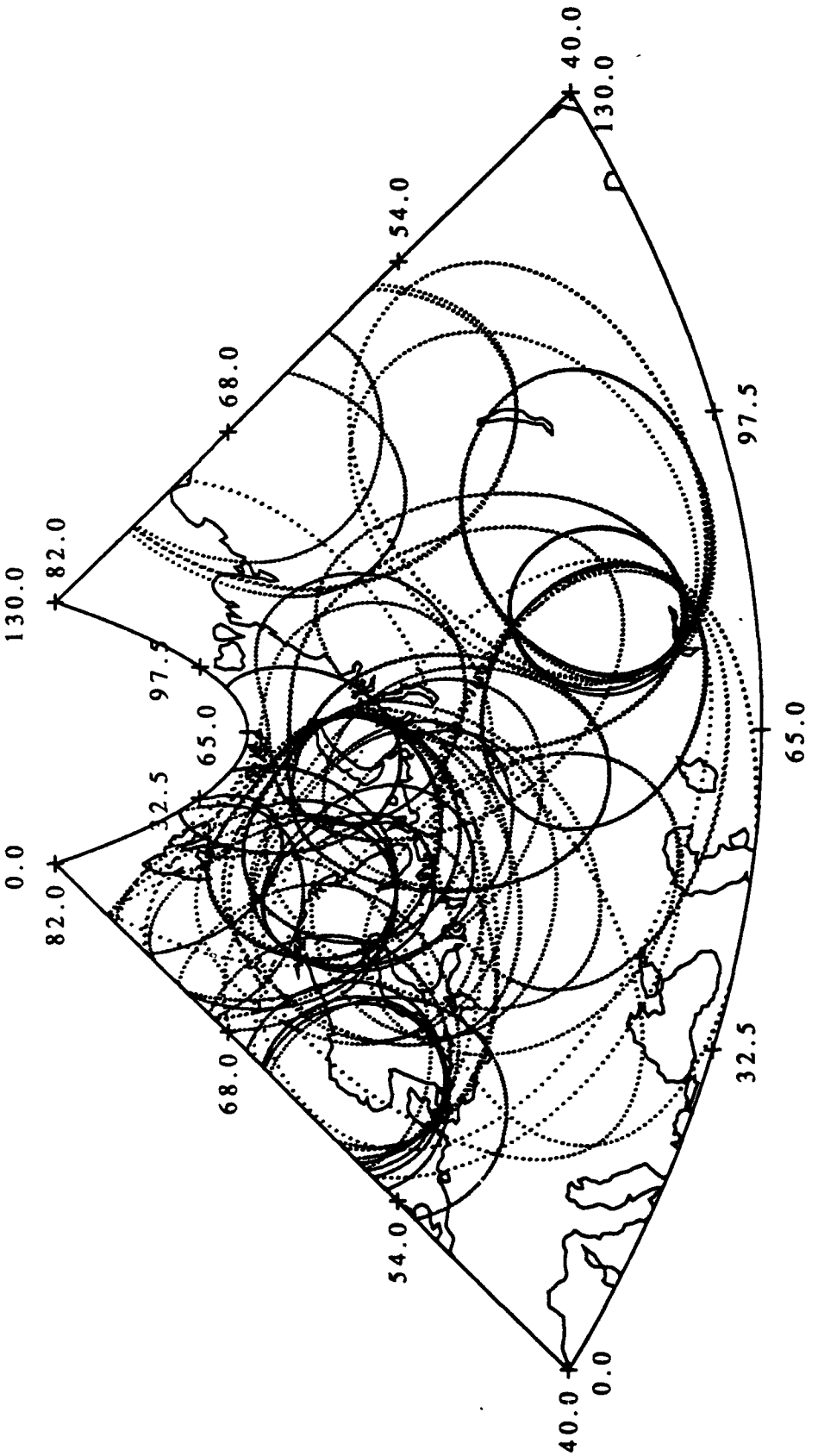
0.0
82.0
130.0
82.0
97.5
65.0
32.5
0.0
40.0
130.0
97.5
65.0
32.5
0.0
40.0
68.0
54.0
68.0
54.0

Figure 1

Attenuation of Multiphase Surface Waves in the Basin and Range Province, part II: Fundamental-mode Surface Waves

by

Brian J. Mitchell

J. Xie

and

W. Lin

Department of Earth & Atmospheric Sciences
Saint Louis University
3507 Laclede
St. Louis, MO 63103

SUMMARY

Attenuation coefficient values of fundamental-mode Rayleigh waves determined for four two-station paths across the Basin and Range province fluctuate between about -2.0×10^{-3} km^{-1} and $+3.0 \times 10^{-3}$ km^{-1} at periods between 6 and 33 s. Particle motion plots indicate that many of those determinations are contaminated by arrivals from non-great circle paths and from waves generated at heterogeneities along the path. Attenuation coefficient determinations for the path MNV to ELK, which is approximately normal to structural trends in that region, are, however, relatively free from such contamination. Mean values for that path decrease rapidly with period from about 3.0×10^{-3} to about 0.7×10^{-3} km^{-1} between 6 and 10 s and then decrease slowly to about 0.3×10^{-3} km^{-1} at 33 s. Standard deviations range between 0.2×10^{-3} and 0.3×10^{-3} km^{-1} for most of the period range, but increase to about 0.4×10^{-3} at periods between 6 and 8 s. These results indicate that careful screening, based upon criteria such as three-dimensional particle motion, are necessary if surface wave attenuation data of sufficient quality to use for inverting for crustal anelasticity in complex regions are to be obtained.

1. INTRODUCTION

This is the second part of a study of the attenuation of surface waves in the Basin and Range province of the western United States. Part I (Xie and Mitchell, 1990) concentrated on the Lg phase and its coda at frequencies between about 0.1 and 10.0 Hz and investigated the effects of ambient noise, station site response, and focussing on Q values measured for those waves. The present paper looks at fundamental-mode surface waves at frequencies between about 0.03 and 0.30 Hz (or periods between about 3 and 30 s). We will assess the usefulness of those waves to study crustal structure in a region containing major lateral structural complexities.

Studies of regional surface wave attenuation became possible over three and a half decades ago with the development of a method to measure the spectral decay of surface wave amplitudes between two points on the Earth's surface (Sato, 1955). Ten years later, Anderson *et al.* (1965) developed a relationship by which attenuation of surface wave amplitudes could be related to anelastic properties of the crust and mantle as a function of depth if the elastic properties are known. A formal process for formally inverting attenuation data, using those relationships and observed attenuation data, was developed using stochastic inversion theory (Mitchell, 1973). Since then, surface wave attenuation values have been measured, and internal friction models have been obtained, for several continental regions (e.g. Mitchell, 1975, 1980, 1981; Hwang and Mitchell, 1987; Cong and Mitchell, 1988; Al-Khatib and Mitchell, 1991). The attenuation coefficient values in these studies typically exhibit very large scatter which has been attributed to arrivals from non-great circle path directions between the source and one or both of the stations. The purpose of this paper is to investigate the severity of those effects on attenuation coefficient determinations over relatively short paths in the western United

States. We will investigate the extent to which attenuation coefficient values obtained in that region are adversely affected by lateral changes in structure and attempt to separate those data which can be reliably used to invert for Q structure from those which are too contaminated to be useful.

2. REGION OF STUDY

We ultimately want to be able to use surface-wave attenuation data obtained over two-station paths in the Basin and Range province to invert for crustal shear-wave internal friction (Q_μ^{-1}) in that region. Those inversion results will be presented in part III of this series of three papers. In principle, these measurements should be straight-forward, requiring only that the waves travel from the source along the same approximate great circle azimuth to both stations. The majority of the paths in this study, however, cross a complex series of tectonic features before reaching the first seismic stations (Figure 1). Features in California alone include the Coast Ranges, the Great Valley and the Sierra Nevada. In addition, some events are situated on or outside the coastline of California or Mexico and surface waves from those events may be adversely affected by the transition between oceanic and continental structure. At best, these features simply contribute a random degree of uncertainty to determinations of attenuation coefficients of surface waves which traverse them. Greater difficulties may, however, arise from focussing, defocussing, or multipathing which may cause systematic errors in the attenuation coefficient determinations.

It has long been known that departures from great circle paths between epicenters and stations could occur for surface waves which cross from oceanic to continental structure in California (Evernden, 1954). More recently, Tanamoto (1990) showed how surface waves could be deflected by laterally varying structure within California. He successfully modelled dispersion

from a source in southern California to six stations in northern California for which great circle paths were parallel or subparallel to structural trends in the region. Ray paths through the western Sierra Nevada at periods of 20 s were deflected by as much as about 60° westward from the expected great circle path.

In addition to effects produced by lateral changes in velocity modelled by Tanamoto (1990), it is possible that topography and variations in sediment thickness could distort wave forms and amplitudes. Sedimentary basins, such as the Great Valley, are known to have a strong effect on both surface wave velocities (Oliver and Ewing, 1958) and amplitudes (Kijko and Mitchell, 1983). These are known to be as thick as 5 km in portions of the Great Valley (Meltzer *et al.*, 1987).

3. ATTENUATION COEFFICIENTS

Seismograms used in this study were written by broadband instruments of the Nevada Test Site Regional Seismic Network operated by Lawrence Livermore National Laboratory. Table 1 gives locations for the four stations of the network and Figure 1 shows their locations relative to source locations and tectonic features. We determined Rayleigh wave attenuation coefficients (γ_R) for four two-station paths (MNV-ELK, MNV-KNB, KNB-ELK, and LAC-MNV) at periods between 6 and 33 s using

$$\ln(A_2(\omega,r)/A_1(\omega,r))\frac{\sqrt{\sin\Delta_2/\sin\Delta_1}}{r_2-r_1} \qquad (1)$$

where r is epicentral distance in km, Δ is epicentral distance in degrees, A is spectral amplitude, ω is angular frequency, and the subscripts 1 and 2 indicate respectively the nearer and farther stations. Interstation phase and group velocities for these paths and crustal velocity models obtained from the inversion of that data are given in Lin (1989).

Attenuation coefficient values obtained for the path MNV-ELK are listed in Table 2 and are plotted in Figure 2. Those values are relatively consistent from event to event. Mean values decrease rapidly from about 3.5×10^{-3} km^{-1} to about 0.7×10^{-3} km^{-1} at periods between 6 and 10 s and decrease slowly to about 0.3×10^{-3} at 33 s. Data for the three other paths (Figure 3), however, exhibit larger scatter, being especially severe for the paths LAC-MNV and KNB-ELK. The large scatter in the plotted values of the Rayleigh wave attenuation coefficients indictes that lateral complexities in the region of study have caused severe distortion to the surface wave amplitudes and that it would be fruitless to try to invert all of the data for anelastic structure. It might also be possible that the consistency of the MNV-ELK data is illusory, and that the data are all adversely affected by lateral complexities in the same systematic manner. We propose to attempt to explain the large scatter in the data apparent in Figure 3 and to investigate the suitability of the MNV-ELK data for inverting for models of crustal anelasticity.

4. SURFACE WAVE PARTICLE MOTION

The determination of surface wave attenuation coefficients using two-station methods and equation (1) assumes that the waves arrive at both stations along approximately the same great circle azimuth from the source. Significant departures from great circle path propagation will mean that amplitude measurements will not be true radial (for Rayleigh waves) or true transverse (for Love waves) motion in the horizontal plane. A more serious problem is that arrivals at two stations from two different non-great circle paths will have left the earthquake focal region at different azimuths. If the source radiation pattern varies rapidly with azimuth, the amplitude differences recorded at two stations will be affected by differences in azimuthally-variable source amplitudes more strongly than by attenuation along the path.

We have estimated the angles of departure from great circle paths for all of the three-component data available to us by calculating three-dimensional particle motion for the surface waves for various velocity windows. An example appears in Figure 4 for three components of ground motion measured at station ELK for the earthquake of 25 September 85 which occurred near the coast of Mexico (Figure 1). The great circle path between the earthquake and ELK is 2769 km in length and passes through and near part of the western boundary of the Sierra Madre Occidental. The horizontal components were rotated to obtain radial and transverse ground motion with respect to the great circle path. Particle motion was determined for five time windows corresponding to group velocities between 3.46 and 3.08 km/s, velocities which are expected for Love waves in this region. The particle motion diagrams for windows 2 through 4 indicate predominantly horizontal motion. These windows therefore have recorded Love waves, but the angle of approach deviates greatly from a great circle path. Windows 2 through 4 indicate that the Love waves arrive at station ELK at 45–60° to the west from the great circle direction. These angles suggest that the waves have arrived after having been laterally refracted or reflected from a feature to the west. Since the travel times are not obviously larger than expected, that feature is not far away and is probably the Sierra Nevada rather than anything further to the west. This is consistent with the plots of Tanamoto (1990) which show large deflections produced by the Sierra Nevada to stations in the other direction from that range. Figure 5 shows the same seismograms and particle motion diagrams for the Rayleigh wave window between 3.01 and 2.71 km/s. This motion is less ordered than that for the earlier Love waves, but windows 2 through 4 indicate Rayleigh motion which deviates greatly from a great circle path direction. Window 2 displays the only ground motion for which an

azimuthal estimate can be made; motion in the horizontal plane suggests an arrival from the west at an angle of about 90° to the great circle path. This direction and the observed velocities again suggest that these waves have been strongly deflected eastward by the Sierra Nevada.

Figure 6 shows seismograms written at station LAC from an earthquake which occurred on 8 May 1985 in the northern part of Baja California, about 300 km south of the station. Particle motion was plotted for five velocity windows between 3.32 and 2.14 km/s. Window 1 shows ground motion corresponding to Love waves arriving along an approximate great circle path from the source; particle motion is predominantly horizontal and at right angles to the direction of propagation. Windows 2 and 3 show ground motion corresponding to Rayleigh waves arriving along an approximate great circle path. Window 2 indicates that particle motion is predominantly radial in the horizontal plane and retrograde-elliptical in the sagittal plane. Horizontal particle motion in window 3 departs by about 30° from the great circle. This departure is caused by a component of Love wave motion on the transverse component which is relatively large for this time window. Windows 4 and 5 display more erratic motion, with a small Rayleigh wave component, indicating that energy from non-great circle paths dominates the ground motion in this interval.

Seismograms from the same earthquake (8 May 1985) recorded at station MNV, 772 km from the source, appear in Figure 7. Particle motion is plotted for five velocity windows between 3.30 and 2.72 km/s. Windows 1 and 2 are dominated by Love wave motion arriving at azimuths which deviate between 40 and 45° westward from the great circle azimuth from the source. As for the event of 25 September 1985, these appear to have been deflected by the Sierra Nevada. Rayleigh motion dominates window 3 and arrives from an

approximate great circle path in this small interval. These seismograms indictae that Love waves and Rayleigh waves are affected differently for this path. Later arriving energy (windows 4 and 5) retain a suggestion of Rayleigh motion, but are too contaminated by incoherent arrivals to be useful for studying crustal anelasticity.

Figure 8 displays seismograms recorded at station MNV from an earthquake in central California which occurred on 9 July 1983 and particle motion for five velocity windows between 2.86 and 1.97 km/s. All windows indicate Rayleigh motion, being predominantly radial in the horizontal plane and retrograde elliptical in the sagittal plane. The departures from the radial direction are small and can be explained as being caused by a component of Love wave motion which overlaps the Rayleigh arrivals and produces net ground motion which deviates from the great circle path direction.

Figure 9 shows the same seismograms as Figure 8, but the particle motion is plotted for velocities between 1.85 and 1.43 km/s. The particle motion in windows 1 and 2 show erratic Rayleigh motion and windows 3 through 5 indicate Love wave motion from an azimuth which is close to the great circle direction from the source. The measured velocities for those Love waves (1.66 to 1.43 km/s) are much lower than velocities which we would expect for this source location, suggesting that they really originate closer to the station. Using realistic values for interstation group velocities we can estimate the distance from the first station at which these Love waves were generated. Assuming a value of 3.1 km/s places that distance at 124 km west of station MNV and assuming a value of 2.8 places it at 138 km west of MNV. The Love waves in the late portions of these seismograms therefore appear to have been generated at, or near, the eastern margin of the Sierra Nevada.

Whether or not Love waves are generated along the propagation path

appears to be very sensitive to the azimuth at which the Rayleigh waves traverse the Sierra Nevada. Figure 10 shows two sets on 3-component seismograms recorded at station MNV. One set is the same as that in Figure 8 and 9. The other is for the event of 9 September 1983 which was located about 8 km closer to station MNV and for which the great circle azimuth (218°) differs from that of the previous event (220°) by only 2°. Note that whereas the transverse record for the event of 9 July contains a high level of Love wave energy late in the wave train, little or no Love wave energy is present in that portion of the transverse record for the event of 9 September. This difference in the level of Love wave energy occurs even though the Rayleigh waves on the vertical and radial components are not greatly different.

5. DISCUSSION

The particle motion plots in Figures 4, 5, and 7 indicate that some surface wave data is affected by arrivals from paths which deviate from a great circle, sometimes by a large amount. This is especially true for paths which are sub-parallel to the major structural trends in our region of study. Those data are likely to produce biased attenuation coefficient values and should not be used to infer models of internal friction. In addition, some seismograms for paths which are at near normal incidence to the Sierra Nevada include path-generated waves. In the present study, however, they are late in the wave trains and do not adversely affect the portions of the seismograms used for attenuation coefficient determinations.

The path MNV-ELK provides a consistent set of attenuation coefficient values. This path, being nearly normal to the structural trends of the region of study, yields particle motion diagrams which indicate pure Rayleigh motion in the radial direction over at least the early part of the Rayleigh wave train. The data for the path MNV-ELK will be used in part III to invert for

crustal anelasticity in the Basin and Range province.

6. CONCLUSIONS

Particle motion diagrams for surface waves in the western United States often reveal complex motion which is produced by lateral complexities in structure. The most severe distortions from expected Love or Rayleigh wave motion occur for long paths which pass through the Sierra Nevada in a direction subparallel to its trend. The Sierra Nevada deflects seismic waves in the present study up to 90° and can deflect Love waves and Rayleigh waves by different amounts. Rayleigh motion is converted to Love motion near the eastern margin of the Sierra Nevada for some events but not others, even though the events are not far from one another, suggesting that mode conversion is very sensitive to the angle at which the waves arrive at that margin. If surface waves are to be utilized to invert for anelastic structure, they should be scrutinized carefully to make sure that their particle motion corresponds to Rayleigh or Love wave motion on a great circle path between the event and recording stations. Such screening has produced a consistent data set, with relatively small standard deviations, for a path across the Basin and Range province.

ACKNOWLEDGMENTS

We thank Bill Tapley and Steve Taylor at the Lawrence Livermore Laboratory for help in acquiring the data for this study. The original version of the particle motion program we used was written by Batakrishna Mandal. This research was supported by the Defense Advanced Research Projects Agency of the Department of Defense under contract FY29601-91-K-DB19.

REFERENCES

Al-Khatib, H.H. and Mitchell, B.J., 1991. Upper mantle anelasticity and tectonic evolution of the western United States from surface wave attenuation, *J. Geophys. Res.*, *96*, 18,129-18,146.

Anderson D.L., Ben-Menahem A., and Archambeau, C.B., 1965. Attenuation of seismic energy in the upper mantle, *J. Geophys. Res. 70*, 1441-1448.

Cong L., and Mitchell, B.J., 1988. Frequency dependence of crustal Q_β in stable and tectonically active regions, *PAGEOPH, 127*, 581-605.

Evernden, J.F., 1953. Direction of approcah of Rayleigh waves and related problems (part I), *Bull. Seism. Soc. Am.*, *43*, 335-353.

Evernden, J.F., 1954. Direction of approach of Rayleigh waves and related problems (part II), *Bull. Seism. Soc. Am.*, *44*, 159-184.

Franklin, J.N., 1970. Well-posed stochastic extensions of ill-posed linear problems, *J. Math. Analysis Applic.*, *31*, 682-716.

Hwang, H.J., and Mitchell, B.J., 1987. Shear velocities, Q_β, and the frequency dependence of Q_β in stable and tectonically active regions from surface wave observations, *Geophys. J.R. Ast. Soc.*, *90*, 575-613.

Kijko, A., and Mitchell, B.J., 1983. Multimode Rayleigh wave attenuation and Q_β in the crust of the Barents shelf, *J. Geophys. Res.*, *88*, 3315-3328.

Lin, W.J., 1989. Rayleigh wave attenuation in the Basin and Range province, M.S. Thesis, Saint Louis University, 55 pp.

Meltzer, A.S., Levander, A.R., and Mooney, W.D., 1987. Upper crustal structure, Livermore Valley and vicinity, California coast ranges, *Bull. Seism. Soc. Am.*, *77*, 1655-1673.

Mitchell, B.J., 1973. Surface wave attenuation and crustal anelasticity in central North America, *Bull. Seism. Soc. Am.*, *63*, 1057-1071.

Mitchell, B.J., 1975. Regional Rayleigh wave attenuation in North America, *J. Geophys. Res.*, *80*, 4904-4916.

Mitchell, B.J., 1980. Frequency dependence of shear wave internal friction in the crust of eastern North America, *J. Geophys. Res.*, *85*, 5212-5218.

Mitchell, B.J., 1981. Regional variation and frequency dependence of Q in the crust of the United States, *Bull. Seism. Soc. Am.*, *71*, 1531-1538.

Oliver, J., and Ewing M., The effect of surficial sedimentary layers on continental surface waves, *Bull. Seism. Soc. Am.*, *48*, 339-354.

Satô, Y., 1955. Analysis of dispersal surface waves by means of Fourier transform I, *Bull. Earthquake Res. Inst.*, *33*, 33-48.

Tanimoto, T., 1990. Modelling curved surface wave paths: membrane surface wave synthetics, *Geophys. J. Int.*, *102*, 89-100.

Xie, J., and Mitchell, B.J., 1990. Attenuation of multiphase surface waves in the Basin and Range province, part I: Lg and Lg coda, *Geophys. J. Int.*, *102*, 121-137.

TABLE 1

Station Codes and Locations

Code	Location	Degrees Latitude	Degrees Longitude
ELK	Elko, NV	40.7448N	115.2388W
KNB	Kanab, UT	37.0166N	112.8224W
LAC	Landers, CA	34.3898N	116.4115W
MNV	Mina, NV	38.4322N	118.1544W

Table 2

Earthquake Location Parameters
(from PDE Monthly Listings)

Date	Origin Time h m s	Latitude (N)	Longitude (W)	Depth (km)	m_b	Two-station Path
24 Sep 80	08 08 38.9	36.27	120.17	9	4.8	MNV-ELK
9 May 83	20 09 15.4	19.98	109.45	10	5.5	LAC-MNV
22 May 83	08 39 21.4	36.14	120.22	10	4.2	MNV-ELK
29 May 83	06 55 33.1	40.46	125.44	10	5.1	MNV-KNB
7 Jun 83	05 18 37.4	36.14	120.24	10	4.2	MNV-ELK
9 Jul 83	07 40 50.9	36.24	120.41	10	5.3	MNV-ELK
22 Jul 83	02 39 53.7	36.23	120.42	9	6.0	MNV-ELK
22 Jul 83	03 43 00.6	36.21	120.41	10	5.3	MNV-ELK
25 Jul 83	22 31 39.2	36.22	120.41	10	5.6	MNV-ELK
09 Sep 83	09 16 14.9	36.23	120.26	5	5.3	MNV-ELK
11 Sep 83	11 48 08.0	36.23	120.39	8	5.0	MNV-ELK
4 Aug 84	21 45 52.9	40.25	124.61	5	4.7	MNV-KNB
8 May 85	23 40 18.2	31.74	115.81	6	5.1	LAC-MNV
10 May 85	05 39 36.3	31.71	115.77	6	4.6	LAC-MNV
12 May 85	13 55.08.2	40.38	125.18	10	4.6	MNV-KNB
21 Sep 85	01 37 13.4	17.80	101.65	31	6.3	KNB-ELK
25 Sep 85	07 43 57.0	18.21	102.74	30	5.3	KNB-ELK

FIGURE CAPTIONS

Figure 1. Map showing source locations, seismic stations, and great circle paths between them. Heavy lines denote approximate boundaries of tectonic provinces traversed by the surface waves.

Figure 2. Fundamental-mode Rayleigh wave attenuation coefficient values for the paths LAC-MNV, MNV-KNB, and KNB-ELK. The solid line indicates average values for the path MNV-ELK and vertical bars denote standard deviations.

Figure 3. Fundamental-mode Rayleigh wave attenuation coefficient values for the path MNV to ELK.

Figure 4. Seismograms for the earthquake of 25 September 1985 recorded at station ELK with particle motion plotted over the Love wave velocity interval between 3.46 and 3.08 km/s. The vertical lines below the seismograms indicate time windows for each of the particle motion plots. Window numbers appear above the particle motion plots in the horizontal, sagittal, and vertical (in the direction of propagation) planes and the corresponding velocity windows are given to the left of the seismograms. The number by each diagram gives the maximum relative motion for the corresponding window. The arrows on the axes of the horizontal and sagittal plots denote the expected direction for great circle propagation.

Figure 5. Seismograms for the earthquake of 25 September 1985 recorded at station ELK with particle motion plotted over the Rayleigh wave velocity interval between 3.01 and 2.71 km/s. See the caption for Figure 4 for an explanation of details of the plot.

Figure 6. Seismograms for the earthquake of 8 May 1985 recorded at station LAC. The seismograms are band-pass filtered between 3 and 30 s using a 5-pole Butterworth filter and particle motion is plotted over the velocity interval between 3.32 and 2.14 km/s. See the caption for Figure 4 for an explanation of the details of the plot.

Figure 7. Seismograms for the earthquake of 8 May 1985 recorded at station MNV. The seismograms are band-pass filtered between 3 and 30 s using a 5-pole Butterworth filter and particle motion is plotted over the velocity interval between 3.30 and 2.72 km/s. See the caption for Figure 4 for an explanation of the details of the plot.

Figure 8. Seismograms for the earthquake of 9 July 1983 recorded at station MNV. The seismograms are band-pass filtered between 3 and 30 s using a 5-pole Butterworth filter and particle motion is plotted over the velocity interval between 2.86 and 1.97 km/s. See the caption for Figure 4 for an

explanation of the details of the plot.

Figure 9. Seismograms for the earthquake of 9 July 1983 recorded at station MNV. The seismograms are band-pass filtered between 3 and 30 s using a 5-pole Butterworth filter and particle motion is plotted over the velocity interval between 1.85 and 1.43 km/s. See the caption for Figure 4 for an explanation of the details of the plot.

Figure 10. Comparison of seismograms from the earthquake of 9 July 1983 with those of 9 September 1983 recorded at station MNV.

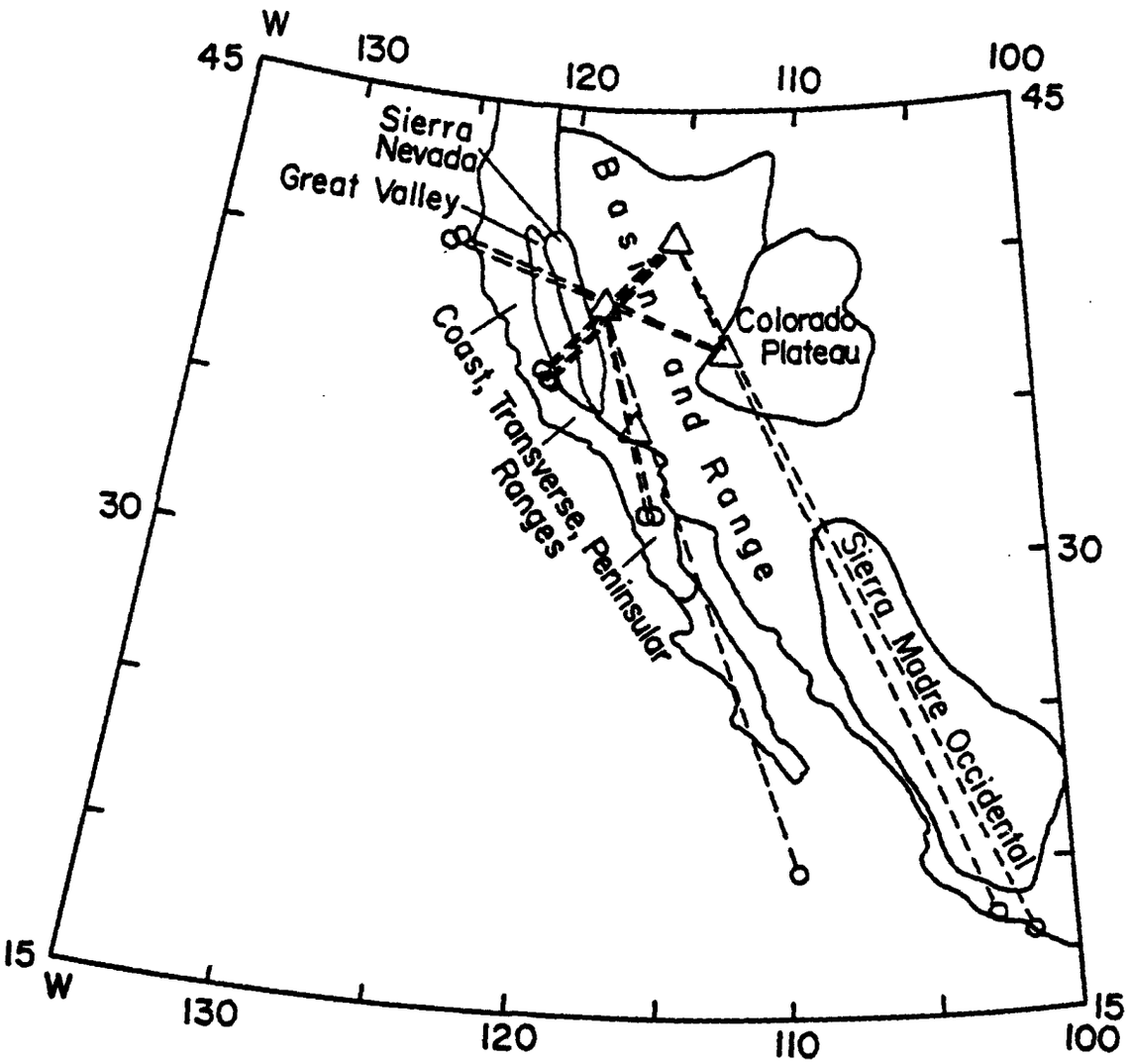
W
45
130
120
110
100
45
Sierra
Nevada
Great Valley
Basin and Range
Colorado
Plateau
Coast, Transverse, Peninsular
Ranges
Sierra Madre Occidental
30
30
15
W
130
120
110
100
15

Figure 1

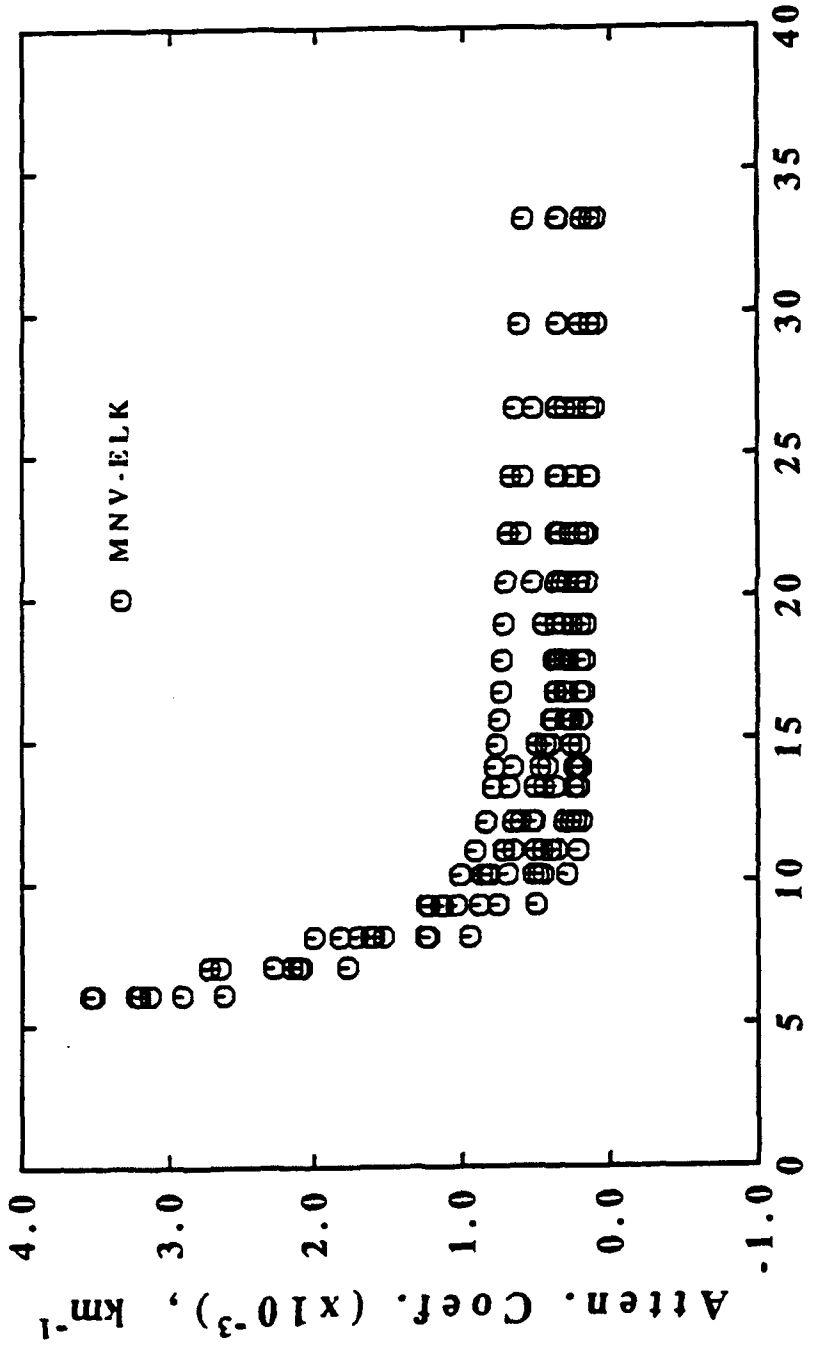
MNV-ELK
Atten. Coef. (x10^{-3}), km^{-1}
4.0
3.0
2.0
1.0
0.0
-1.0
0
5
10
15
20
25
30
35
40
Period, sec

Figure 2

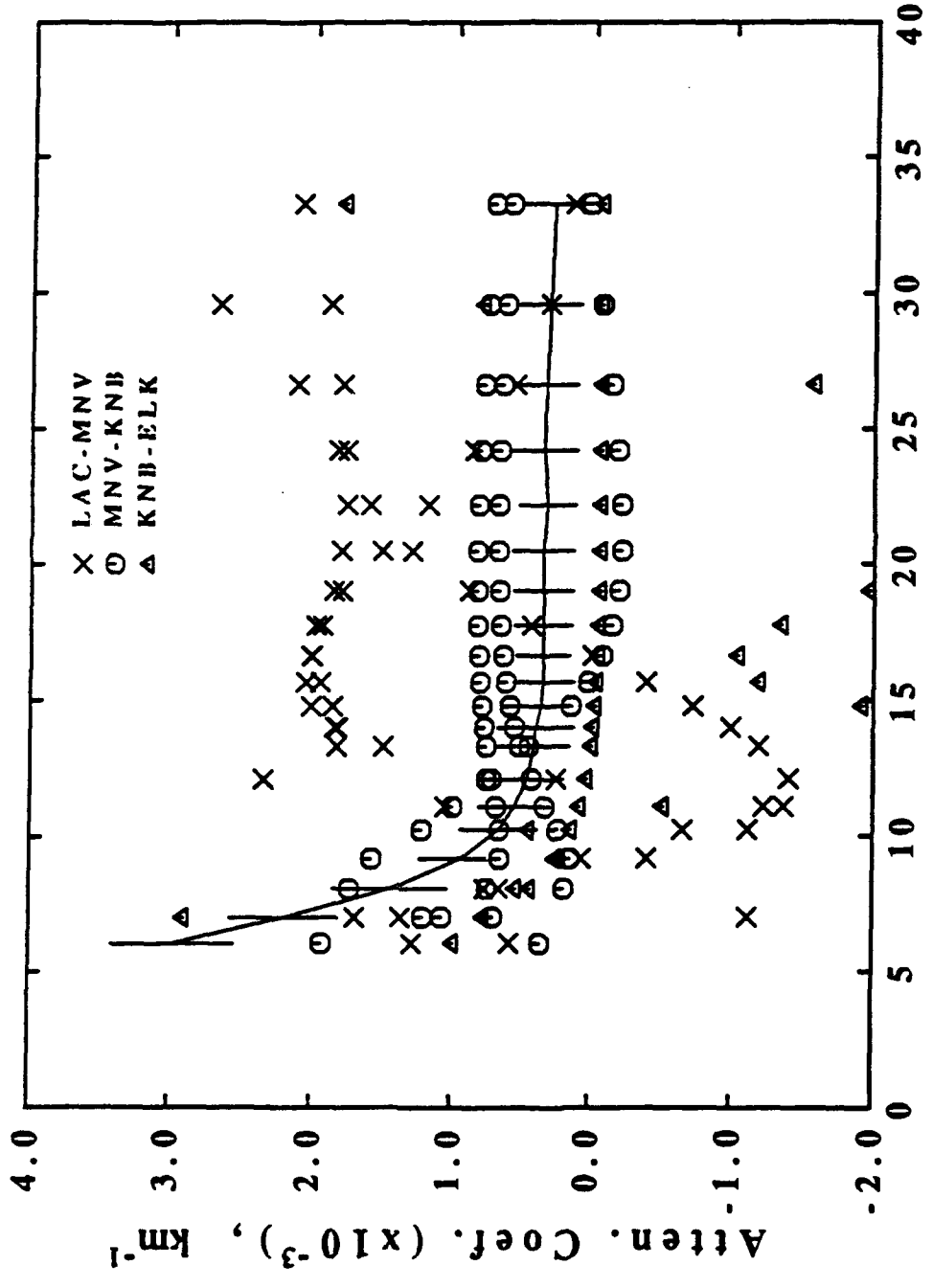
LAC-MNV
MNV-KNB
KNB-ELK
Period, sec
0
5
10
15
20
25
30
35
40
4.0
3.0
2.0
1.0
0.0
-1.0
-2.0
Atten. Coef. (x10⁻³), km⁻¹

Figure 3

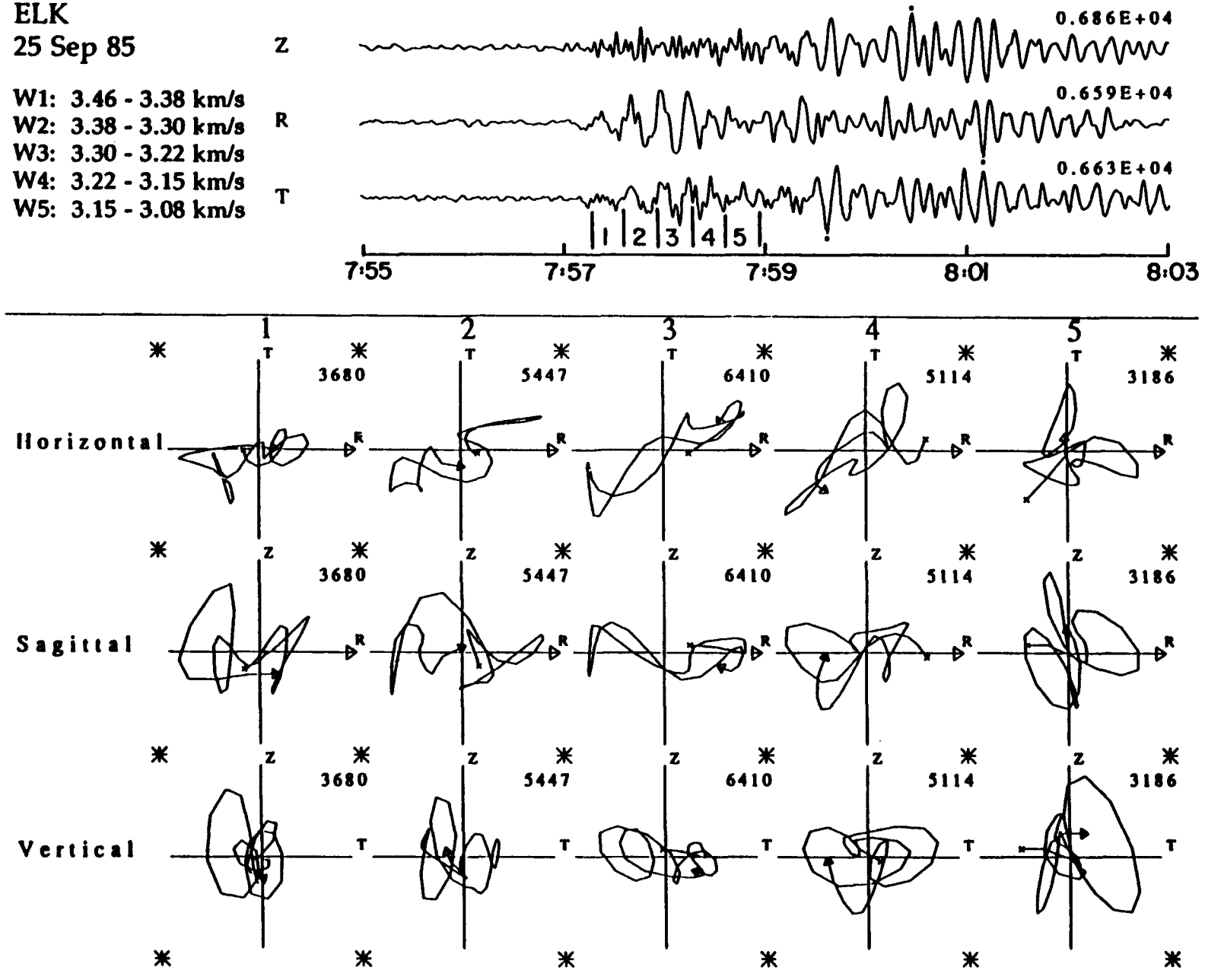
ELK
25 Sep 85
W1: 3.46 - 3.38 km/s
W2: 3.38 - 3.30 km/s
W3: 3.30 - 3.22 km/s
W4: 3.22 - 3.15 km/s
W5: 3.15 - 3.08 km/s
Z
R
T
0.686E+04
0.659E+04
0.663E+04
1 2 3 4 5
7:55
7:57
7:59
8:01
8:03
Horizontal
Sagittal
Vertical
3680
5447
6410
5114
3186

Figure 4

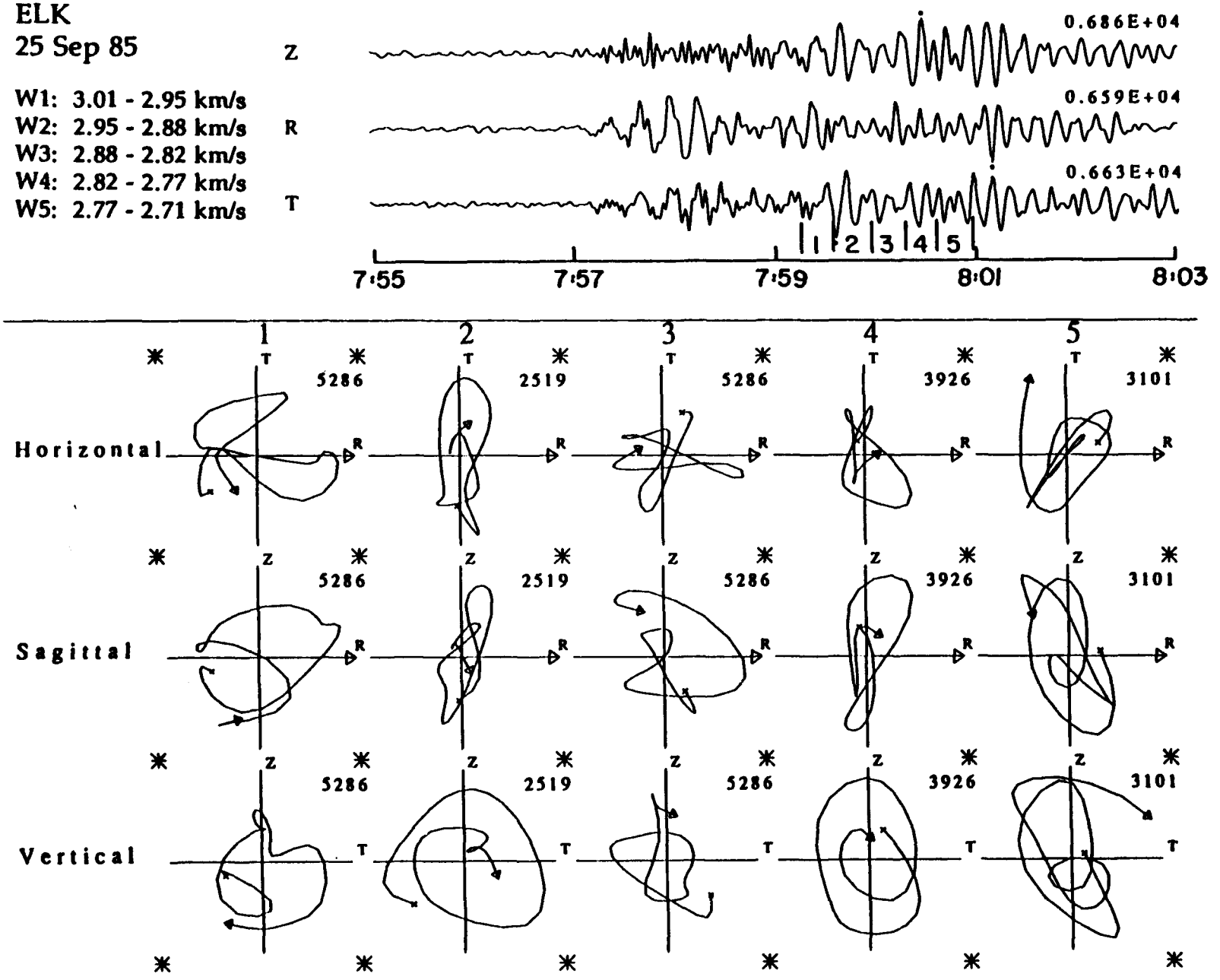
ELK
25 Sep 85
W1: 3.01 - 2.95 km/s
W2: 2.95 - 2.88 km/s
W3: 2.88 - 2.82 km/s
W4: 2.82 - 2.77 km/s
W5: 2.77 - 2.71 km/s
Z
R
T
0.686E+04
0.659E+04
0.663E+04
1 2 3 4 5
7:55
7:57
7:59
8:01
8:03
Horizontal
Sagittal
Vertical
5286
2519
5286
3926
3101

Figure 5

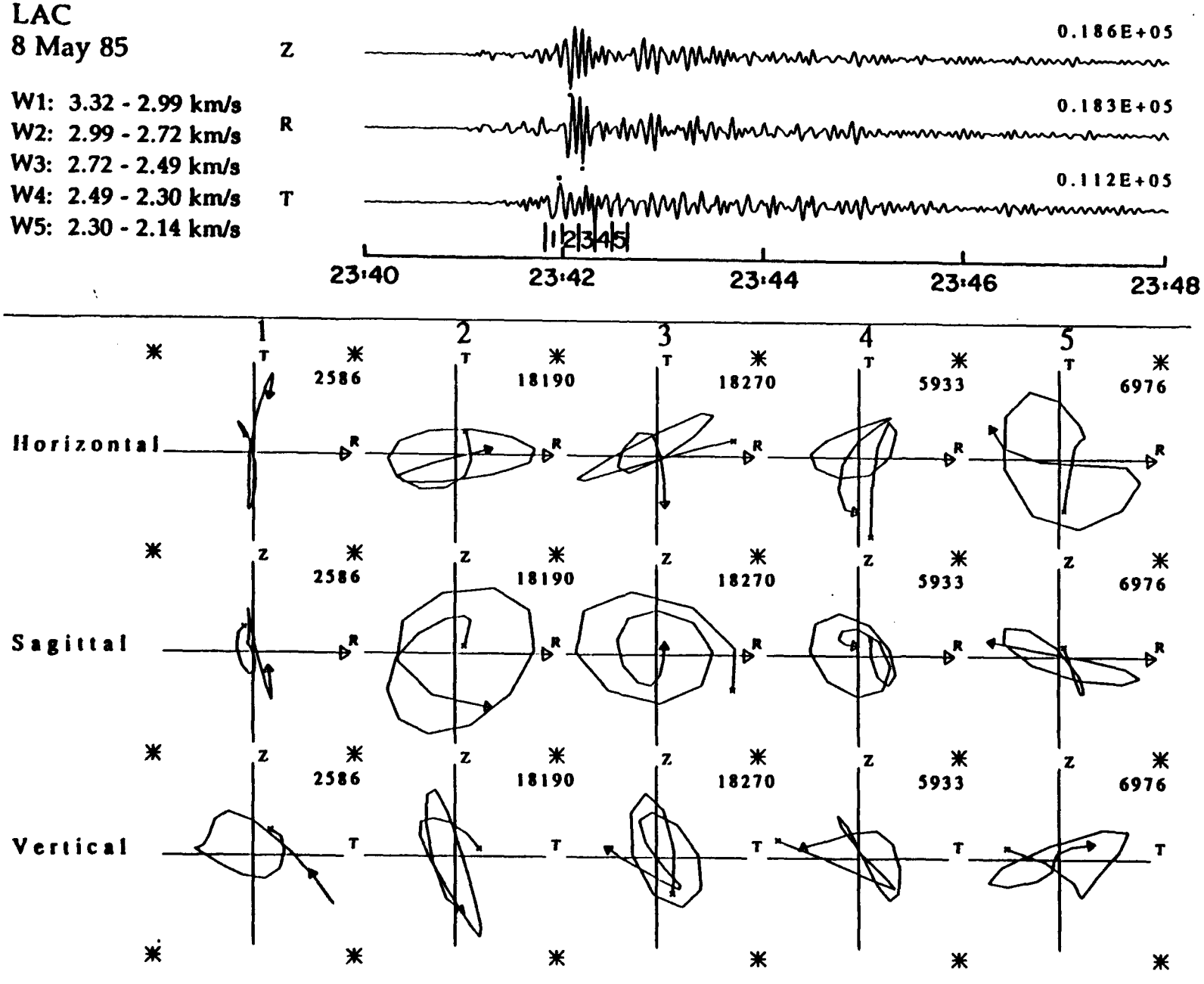
LAC
8 May 85
W1: 3.32 - 2.99 km/s
W2: 2.99 - 2.72 km/s
W3: 2.72 - 2.49 km/s
W4: 2.49 - 2.30 km/s
W5: 2.30 - 2.14 km/s
Z
R
T
0.186E+05
0.183E+05
0.112E+05
1 2 3 4 5
23:40
23:42
23:44
23:46
23:48
1
2
3
4
5
2586
18190
18270
5933
6976
Horizontal
Sagittal
Vertical

Figure 6

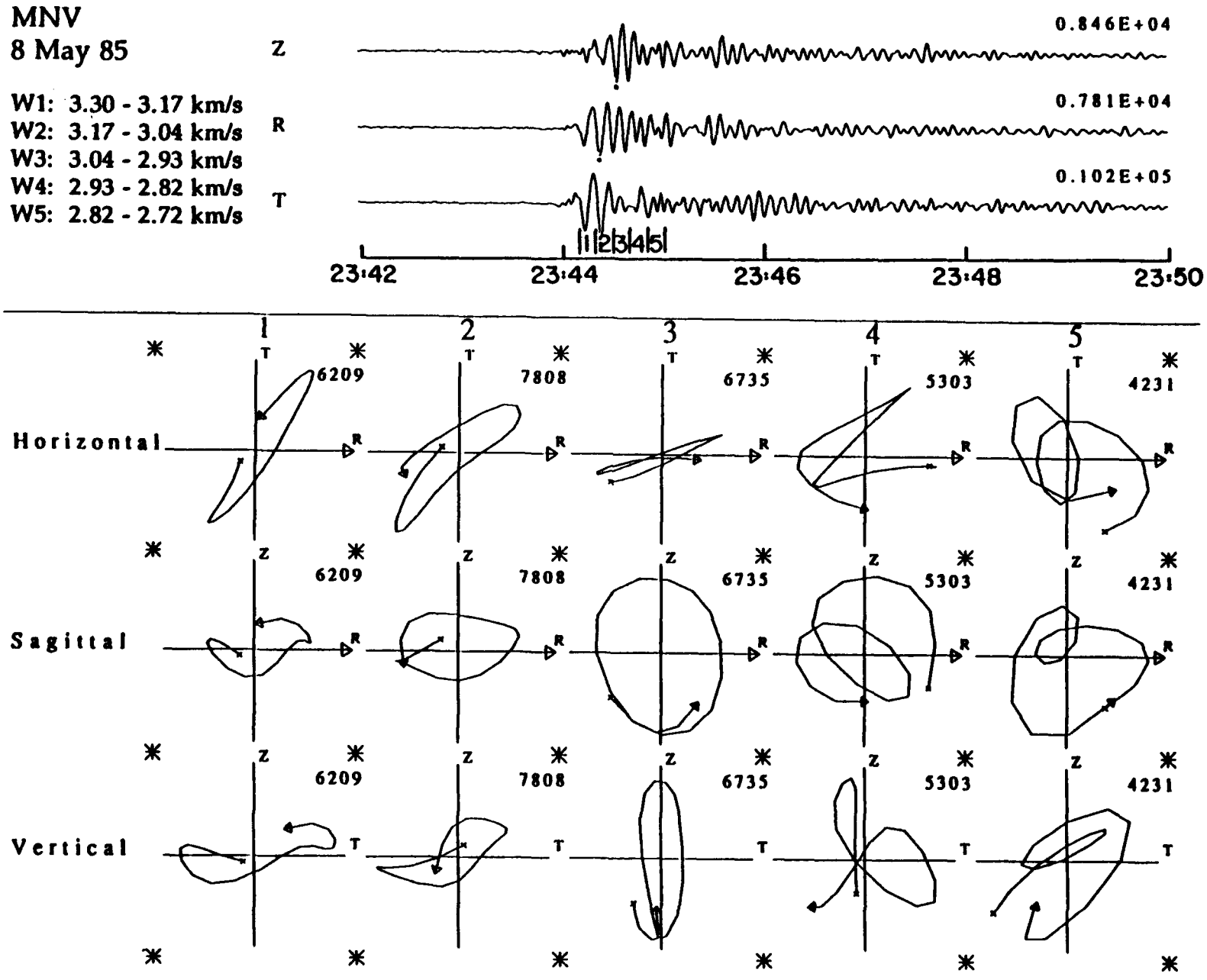
MNV
8 May 85
W1: 3.30 - 3.17 km/s
W2: 3.17 - 3.04 km/s
W3: 3.04 - 2.93 km/s
W4: 2.93 - 2.82 km/s
W5: 2.82 - 2.72 km/s
Z
R
T
0.846E+04
0.781E+04
0.102E+05
1 2 3 4 5
23:42
23:44
23:46
23:48
23:50
Horizontal
Sagittal
Vertical
6209
7808
6735
5303
4231

Figure 7

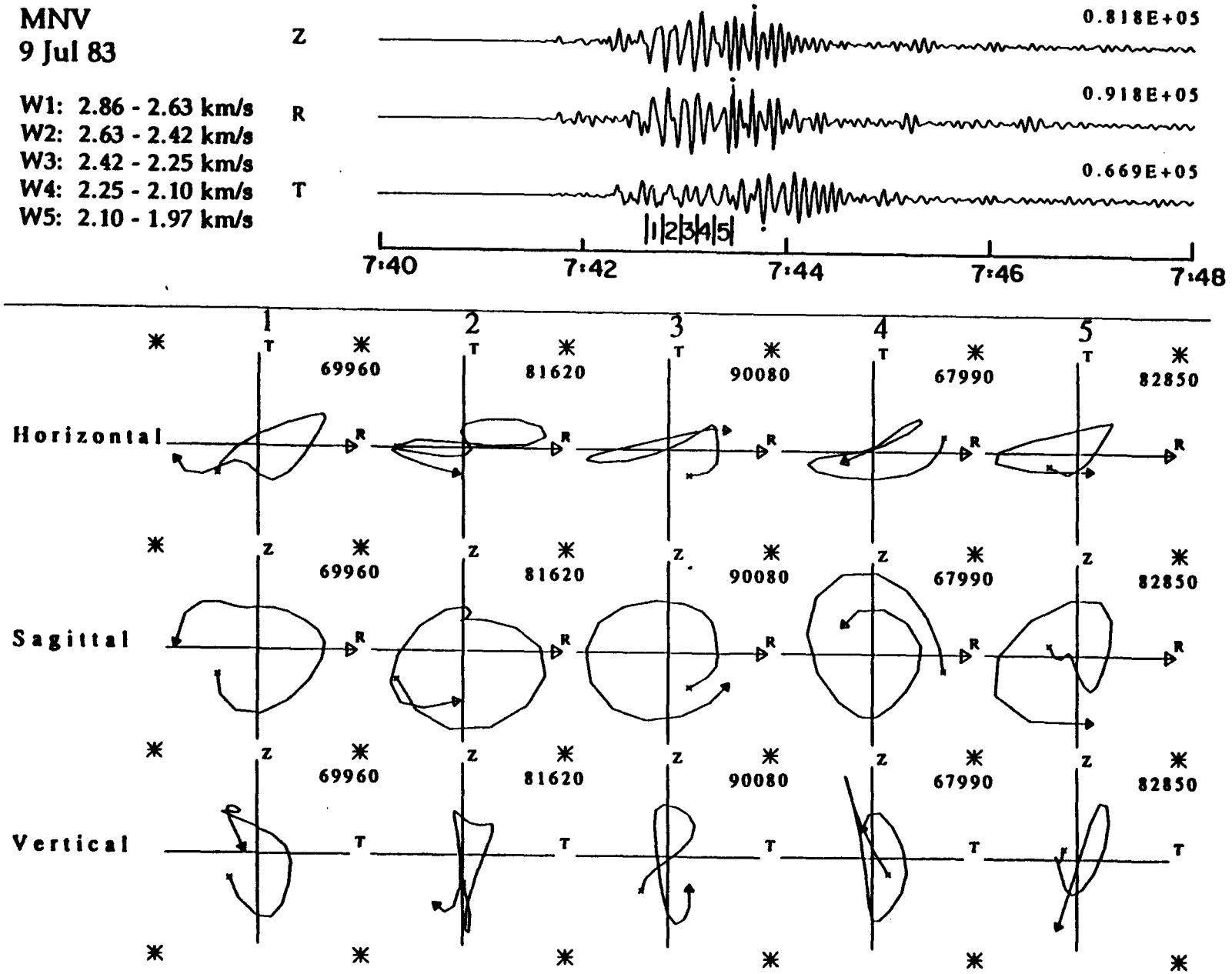
MNV
9 Jul 83
W1: 2.86 - 2.63 km/s
W2: 2.63 - 2.42 km/s
W3: 2.42 - 2.25 km/s
W4: 2.25 - 2.10 km/s
W5: 2.10 - 1.97 km/s
Z
R
T
0.818E+05
0.918E+05
0.669E+05
1 2 3 4 5
7:40
7:42
7:44
7:46
7:48
Horizontal
Sagittal
Vertical
69960
81620
90080
67990
82850

Figure 8

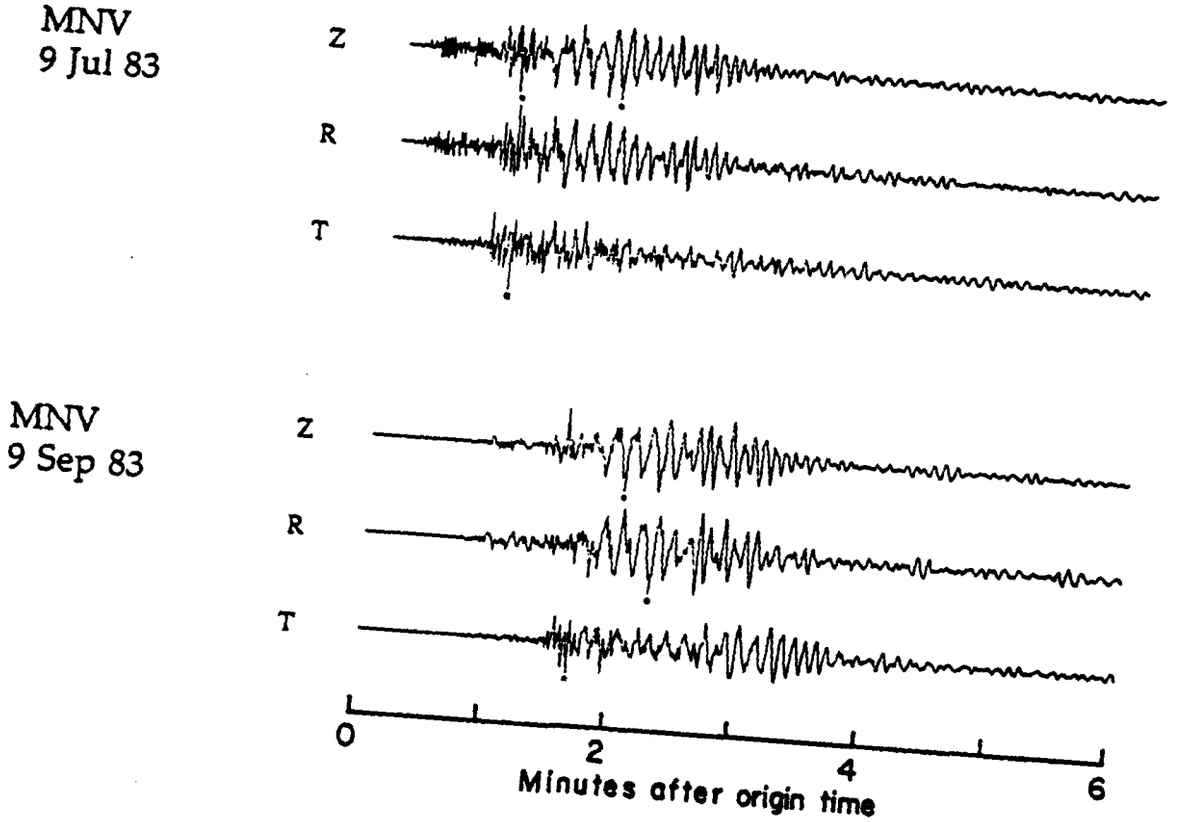
MNV
9 Jul 83
Z
R
T
MNV
9 Sep 83
Z
R
T
0
2
4
6
Minutes after origin time

Figure 9